efficiency in the different states above the α transition is the difference in the effective end group concentration.

Further work in the high molecular weight range, utilizing samples possessing extremely narrow molecular weight distributions, is clearly necessary in order to substantiate these conclusions. Only when the results of these experiments are available can an unequivocal answer be obtained as to whether there is any direct influence of the drastically different molecular conformations in the two states on the cross-linking process. The results for the lower molecular weight hydrogenated samples argue against any direct influence of conformation at these temperatures. This conclusion is in accord with the results obtained for the irradiation of poly(*trans*-1,4-isoprene) in the crystalline state at 20° and in the completely molten state at 100°.[31]

(31) D. T. Turner, *J. Polym. Sci., Part B*, **4**, 717 (1966).

Molecular Weight Distribution of Polyethylene Produced by Ziegler–Natta Catalysts

Daljit Singh and R. P. Merrill*

Department of Chemical Engineering, University of California,
Berkeley, California 94720. *Received December 10, 1970*

ABSTRACT: The unusually broad molecular weight distribution observed in the Ziegler–Natta polymerization of ethylene is explained by considering the diffusion of monomer and the movement of catalytic sites in a growing polymer particle. An analysis of appropriate mathematical models for various intervals of polymerization indicates that broad molecular weight distributions ($\bar{M}_w/\bar{M}_n > 2$) may be obtained for values of Thiele parameters (based on the size of the polymer particle) greater than about 6. The use of additives which decrease the polymerization rate appears to be a promising method for reducing $\bar{M}_w/\bar{M}_n$. Better solvents and a programmed pressure cycle during polymerization may also be helpful. The anomalies reported in the rates and orders of reaction in literature have been traced to the experimental conditions and are explained in the light of the proposed diffusion analysis.

The polymerization of unsaturated monomers using heterogeneous catalysts has been actively researched in recent years, producing a variety of patented catalysts, most of which contain a transition metal halide (typically $TiCl_4$ or α-$TiCl_3$) and an organometallic compound (generally an alkyl halide or trihalide of aluminum) in various combinations and proportions.[1] This type of catalyst is frequently referred to as a Ziegler–Natta catalyst and has the distinct advantage of being able to polymerize ethylene into a high-molecular-weight, high-density material at low pressures (typically, 1–5 atm). The polyethylene produced by these catalysts is highly linear, having less than 1 side chain per 200 carbon atoms in the backbone chain, and, as a consequence, it possesses better physical and mechanical characteristics (compared to the high-pressure product).[2] However, the polymer has an unusually broad molecular weight distribution[3-5] which adversely effects properties like resistance to environmental stress cracking and crazing.[2] A broad molecular weight distribution also results in melt-processing difficulties. Solid-state properties usually correlate with $\bar{M}_n$, but melt viscosity varies as some power of $\bar{M}_w$. A "high-*M* tail" to the distribution thus makes a disproportionate contribution to viscous drag, power costs, etc. It is therefore of interest to be able to understand the cause of this broad molecular weight distribution and devise techniques for narrowing it.

In the case of homogeneous free-radical or ionic polymerizations, where the mechanism of polymerization is well understood, the molecular weight distribution of polymer can be derived either from the polymerization kinetics or from simple probability arguments. The width of the instantaneous molecular weight distribution, as measured by the ratio of the weight-average to the number-average molecular weight, lies in the range 1.5–2.0,[6] depending upon the predominant mode of termination. Chain-transfer reactions may lead to a value slightly greater than two, but in all cases, the molecular weight distributions are relatively narrow. The distributions derived theoretically are generally in good agreement with the experimental results.

For Ziegler–Natta polymerizations, however, the molecular weight distributions are much broader ($\bar{M}_w/\bar{M}_n$ generally lies between 4 and 40), and the reasons for this are not well understood.[7] For polyethylene, two empirically derived distribution functions have been proposed, both of them having two parameters. The distribution function derived by Tung[3] has the integral form given by

$$I(M) = 1 - \exp(-aM^b) \tag{1}$$

where a and b are empirical parameters and $I(M)$ is the weight fraction of all species having molecular weight less than M. The other distribution function, suggested by Wesslau,[4] is given by

$$I(M) = \frac{1}{\beta\pi^{1/2}}\int_0^M \left(\frac{1}{M}\right) \exp[(-1/\beta^2)(\ln M/M_0)^2]\mathrm{d}M \tag{2}$$

where β and M_0 are the parameters. Equation 2 represents

---

(1) F. W. Breuer, L. E. Giepel, and A. B. Loebel in "Crystalline Olefin Polymers," Part 1, R. A. V. Raff and K. W. Doak, Ed., Interscience, New York, N. Y., 1965, pp 39–90.

(2) F. W. Billmeyer, "Textbook of Polymer Science, "Interscience, New York, N. Y., 1962, pp 363–371.

(3) L. M. Tung, *J. Polym. Sci.*, **20**, 495 (1956).

(4) H. Wesslau, *Makromol. Chem.*, **20**, 111 (1956).

(5) G. K. Williamson, *et al.*, *J. Appl. Chem.*, **14**, 131 (1964).

(6) P. J. Flory, "Principles of Polymer Chemistry," Cornell University Press, Ithaca, N. Y., 1953.

(7) M. N. Berger, G. Boocock, and R. N. Haward, *Advan. Catal.*, **19**, 211 (1969).

Table I
Order of Reaction for Ziegler–Natta Polymerization of α Olefins

Monomer	Reaction order[a]	Ref
Ethylene	1	*b*
Ethylene	1	*c*
Propylene	1	*d*
Ethylene	2	*e*
Ethylene	2	*f*
Ethylene	1–2	*g*
Propylene	1–2	*h*
Propylene	1–2	*i*

[a] With respect to monomer. [b] H. Fielchenfeld and M. Jeselson, *J. Phys. Chem.*, **63**, 720 (1959). [c] D. B. Ludom, A. W. Anderson, and C. E. Ashby, *J. Amer. Chem. Soc.*, **80**, 1380 (1958). [d] Reference 12. [e] J. C. McGowan and B. M. Ford, *J. Chem. Soc.*, 1149 (1958). [f] A. Gilchrist, *J. Polym. Sci.*, **34**, 49 (1959). [g] A. Schindler, *ibid., Part C*, No. **4**, 81 (1964); *Makromol. Chem.*, **70**, 946 (1963). [h] G. Natta, I. Pasquon, J. Swab, and A. Zambelli, *Chem. Ind. (Milan)*, **44**, 621 (1962). [i] K. Vesely, J. Ambroz, and O. Hamrik, *J. Polym. Sci., Part C*, No. **4**, 11 (1963).

a logarithmic normal distribution in which the logarithms of molecular weight are distributed normally about a mean.

In an attempt to understand the cause of this extreme spread in the distribution function and to elucidate the mechanism of Ziegler–Natta-type polymerizations, many kinetic data have been generated, but these data have many inconsistencies in rates and order of reaction. Rates of reaction have been found to increase,[8,9] decrease,[10,11] or remain appreciably constant with time.[12] Order of reaction with respect to monomer has been reported to vary anywhere between one and two.

In Table I are listed some of the reported orders of reaction for ethylene and propylene polymerization in the presence of titanium-based catalyst systems. Neither the probable cause for these inconsistencies in the observed kinetics nor the reasons for the unusually broad molecular weight distribution are known.

It is the purpose of this paper to demonstrate that both these phenomena may occur because of mass-transport limitations within the growing polymer particle. In addition to the usual diffusive transport of monomer, it is also necessary to consider the movement of the active catalytic sites. As the polymer particle grows, the catalyst breaks up into small fragments which are engulfed in the polymer and convected outward.

Mathematical Models

A Ziegler–Natta catalyst is prepared, typically, by reaction of an organometallic compound and a transition metal halide slurried in a dry, oxygen-free inert hydrocarbon solvent such as *n*-heptane. The $TiCl_4$ and organometallic compound are known to react in heptane medium[13] with the formation of a new solid phase containing Ti in its various valence states, Cl, Al, and organic fragments. It is believed that these Ti–Al complexes forming a part of the new solid phase—the exact nature of which is not known as yet—act as catalytic sites for the growth of the polymer. These sites exist as microcrystalline aggregates, slightly greater than 10 μ in diameter.[14] Polymer grows on these sites and in the process breaks these microcrystalline aggregates into smaller fragments which are engulfed by the growing polymer, thereby forming a polymeric core. To a first approximation, the concentration of these sites may be considered nearly uniform and constant. (This concentration is designated by A in the mathematical development which follows.) This assumption is used in the first of the three models, the uniform site concentration (USC) model. After a certain stage when the catalyst pellets have broken up into very small fragments and agglomerated into a polymeric core, no further cleavage takes place and the total number of sites becomes essentially constant in time.

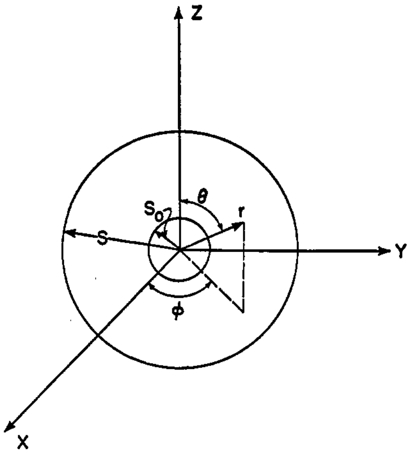

Figure 1. Coordinate system used for polymerization models.

In the second model, the site expansion and conservation (SEC) model, these sites are assumed convected outward with the velocity of the growing polymer, and the appropriate continuity equation is used to describe the motion. The third model, the fixed site model (FSM), analyzes the other limiting case; the sites are assumed to be fixed in a central polymeric core and the polymer builds up as a coating around this core. Though this model is probably not physically representative of the actual polymerization at any stage, it is valuable as a mathematical limit and as such gives some insight into the problem.

(A) Uniform Site Concentration Model. The growing particles are assumed to be spherical in shape and the coordinate system used is shown in Figure 1, where S denotes the radius of the particle at any instant and S_0 represents the radius at zero time. A mass balance on the monomer (assuming spherical symmetry) is given by

$$\frac{\partial C_M}{\partial t} = \frac{D_M}{r^2}\frac{\partial}{\partial r}\left(r^2\frac{\partial C_M}{\partial r}\right) - k_P C_M A - k_T C_M A \qquad (3)$$

Termination is assumed to be by chain transfer to monomer only. Also, monomer addition is assumed to occur only at the site.

The conservation equations for polymer may be written in a similar manner. Separate equations are required for the growing polymer (*i.e.*, a polymer molecule attached to a catalytically active site) and for dead polymer (*i.e.*, a molecule which has undergone a transfer reaction and is not capable of adding another monomer on to it). Equations 4 and 5 de-

---

(8) R. W. Lenz, "Organic Chemistry of Synthetic High Polymers," Interscience, New York, N. Y., 1967.
(9) A. Simon and G. Ghymes, *J. Polym. Sci.*, **53**, 327 (1961).
(10) W. E. Smith and R. E. Zelmer, *ibid., Part A*, **1**, 2587 (1963).
(11) E. Kohn, *et al., ibid.*, **58**, 681 (1962).
(12) G. Natta and I. Pasquon, *Advan. Catal.*, **11**, 1 (1959).
(13) A. Simon, L. Kollár, and L. Böröcz, *Monatsh. Chem.*, **95**, 842 (1964).
(14) T. P. Wilson and G. F. Hurley, *J. Polym. Sci., Part C*, No. **3**, 281 (1963).

note the conservation equations for living and dead i-mers, respectively, having radial velocity, $V_R(r)$.[15]

$$\frac{\partial R_i}{\partial t} = -\frac{1}{r^2}\frac{\partial}{\partial r}(r^2V_RRi) + k_PC_M\,(R_{i-1} - R_i) - k_TC_MR_i \tag{4}$$

$$\frac{\partial P_i}{\partial t} = \frac{1}{r^2}\frac{\partial}{\partial r}(r^2V_RP_i) + k_TC_MR_i \tag{5}$$

In principle, it should be possible to solve eq 3, 4, and 5 for every value of i and thus obtain the complete distribution function. The molecular weight distributions can, however, be obtained in a simplified and straightforward manner by using the method of moments, as suggested by Chiang and Hermans.[16] Equations 6 and 7 define the local nth moment of the living and dead polymer, respectively. Only zero, first,

$$X_n = \sum_{i=0}^{\infty} i^nR_i \tag{6}$$

$$Y_n = \sum_{i=0}^{\infty} i^nP_i \tag{7}$$

and second moments are of relevance for the present purpose. The local moments may be integrated according to eq 8 and 9 to obtain the average over the entire particle

$$X_{n,\mathrm{av}} = \frac{4\pi\int_0^S X_n(r)r^2\mathrm{d}r}{(4/3)\pi S^3} \tag{8}$$

$$Y_{n,\mathrm{av}} = \frac{4\pi\int_0^S Y_n(r)r^2\mathrm{d}r}{(4/3)\pi S^3} \tag{9}$$

The breadth of the molecular weight distribution based on either living or dead polymer may be obtained from the ratio

$$QX_{\mathrm{av}} = \frac{(X_{2,\mathrm{av}})(X_{0,\mathrm{av}})}{(X_{1,\mathrm{av}})^2} \tag{10}$$

$$QY_{\mathrm{av}} = \frac{(Y_{2,\mathrm{av}})(Y_{0,\mathrm{av}})}{(Y_{1,\mathrm{av}})^2} \tag{11}$$

The overall Q factor, based on all the polymer molecules present in the particle, is given by

$$Q_{\mathrm{av}} = \frac{\Sigma_{2,\mathrm{av}}\Sigma_{0,\mathrm{av}}}{(\Sigma_{1,\mathrm{av}})^2} \tag{12}$$

and is a measure of the spread of the molecular weight distribution. In eq 12

$$\Sigma_{n,\mathrm{av}} = X_{n,\mathrm{av}} + Y_{n,\mathrm{av}} \tag{13}$$

In order to obtain the equations for the various moments, eq 4 and 5 are multiplied by i^n and summed over all i. Equations so obtained for zero, first, and second moments are given below.

$$\frac{\partial X_1}{\partial t} = -\frac{1}{r^2}\frac{\partial}{\partial r}(r^2V_RX_1) + k_PC_MA - k_TC_MX_1 \tag{14}$$

$$\frac{\partial X_2}{\partial t} = -\frac{1}{r^2}\frac{\partial}{\partial r}(r^2V_RX_2) + k_PC_M(A + 2X_1) - k_TC_MX_2 \tag{15}$$

$$\frac{\partial Y_0}{\partial t} = -\frac{1}{r^2}\frac{\partial}{\partial r}(r^2V_RY_0) + k_TC_MA \tag{16}$$

$$\frac{\partial Y_1}{\partial t} = -\frac{1}{r^2}\frac{\partial}{\partial r}(r^2V_RY_1) + k_TC_MX_1 \tag{17}$$

$$\frac{\partial Y_2}{\partial t} = -\frac{1}{r^2}\frac{\partial}{\partial r}(r^2V_RY_2) + k_TC_MX_2 \tag{18}$$

It should of course be recognized that $X_0 = A$. Equations 14–18 may be solved for the respective moments and integrated appropriately according to eq 8 and 9, and the Q factors may be computed.

(B) Site Expansion and Conservation Model. The basic equations for the SEC model are the same as those for the USC model. However, A is no longer constant and uniform. Therefore eq 3 and 14–18 have to be solved in conjunction with the continuity equation for the sites, eq 19.

$$\frac{\partial A}{\partial t} = -\frac{1}{r^2}\frac{\partial}{\partial r}(r^2V_RA) \tag{19}$$

(C) Fixed Site Model. In this model one can identify two separate regions—an inner polymeric core with fixed sites and an outer layer with a radial velocity for the polymer. The relevant equations for monomer and site concentration are given below.

$$\frac{\partial C_M}{\partial t} = \frac{D_M}{r^2}\frac{\partial}{\partial r}\left(r^2\frac{\partial C_M}{\partial r}\right) - k_PC_MA - k_TC_MA \qquad 0 < r < S_0 \tag{20}$$

$$\frac{\partial C_M}{\partial T} = \frac{D_M}{r^2}\frac{\partial}{\partial r}\left(r^2\frac{\partial C_M}{\partial r}\right) \qquad S_0 < r < S \tag{21}$$

$$A = A_0 \qquad 0 < r < S_0 \tag{22}$$

$$A = 0 \qquad S_0 < r < S \tag{23}$$

Similar equations can also be written for the living and dead polymers.

$$\frac{\partial R_i}{\partial t} = k_PC_M\,(R_{i-1} - R_i) - k_TC_MR_i \qquad 0 < r < S_0 \tag{24}$$

$$\frac{\partial R_i}{\partial t} = 0 \qquad S_0 < r < S \tag{25}$$

$$\frac{\partial P_i}{\partial t} = k_TC_MR_i \qquad 0 < r < S_0 \tag{26}$$

$$\frac{\partial P_i}{\partial t} = -\frac{1}{r^2}\frac{\partial}{\partial r}(r^2V_RP_i) \qquad S_0 < r < S \tag{27}$$

Equations 24–27 may be multiplied by i^n and summed over i to give equations for the various moments, which, in turn, may be solved for the Q factor.

---

(15) The velocity V_R at any point and instant can be obtained by equating the volumetric rate of formation of polymer product to the rate of growth of the spherical particle.

(16) R. Chiang and J. J. Hermans, *J. Polym. Sci., Part A-1*, **4**, 2843 (1966).

Solution and Results

The equations were all rendered dimensionless and solved numerically by the method of finite differences[17] with the following boundary conditions

$$C_M = C_S \text{ at } r = S$$
$$\frac{\partial C_M}{\partial r} = 0 \text{ at } r = 0 \qquad (28)$$

where C_S is the concentration of monomer in solution, which is assumed constant. It is also assumed that liquid-phase mass transfer is not a controlling step.

The initial profiles of the monomer concentration are depicted in Figure 2 as a plot of the dimensionless monomer concentration, $C_M^* = C_M/C_S$, *vs.* the dimensionless radius, $r^* = r/S_0$, for various values of Thiele parameter, given by

$$Th = \sqrt{\frac{k_P A_0}{D_M}} S_0 \qquad (29)$$

Strictly speaking, in the above definition of the Thiele parameter, $(k_P - k_T)$ should have been used insteady of k_T. However, the solution has been carried out for $k_P/k_T = 10^5$, whence $k_P - k_T \approx k_P$. The conventional pseudo-steady-state assumption was used for solving eq 3.

It is apparent from Figure 2 that for values of the Thiele parameter greater than 25, the monomer concentration declines sharply and falls to an approximate zero value very close to the surface, resulting in a substantial fraction of the sites being deprived of the monomer. As time increases, the concentration curves for all three models shift out to larger values of r^*. The implication is that as the reaction progresses, more and more sites in the core of the growing particle get starved of the monomer and a limited number of sites near the surface get more and more monomer molecules attached to them, resulting in a very broad molecular weight distribution. This is confirmed in Figure 3, where the initial Q factors (at S^* $(=S/S_0) = 1.00625$) are plotted *vs.* the Thiele parameter, showing that diffusional limitation can easily account for the broad molecular weight distributions commonly observed. These initial values of Q are close to the maximum obtainable values. The FSM curve is drawn for the minimum Q factor and as such represents the limiting value of Q attainable in Ziegler–Natta polymerizations (*i.e.*, without any modifications—as discussed in the next section). For values of k_T within a 100-fold range, the Q values lie in a narrow band around the curves of Figure 3. Chain transfer, therefore, does not seem to have an appreciable effect on the $\bar{M}_w/\bar{M}_n$ ratio, as observed earlier by Berger, *et al.*;[7] however, "chain termination" would affect the distribution markedly.

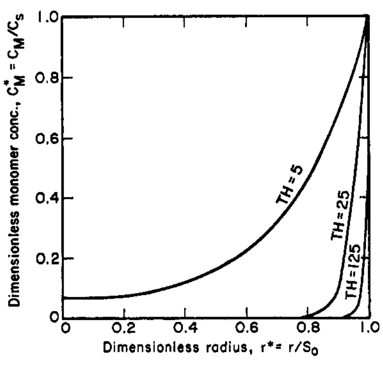

Figure 2. Radial distribution of monomer concentration in polymer particle for various values of the Theile parameter.

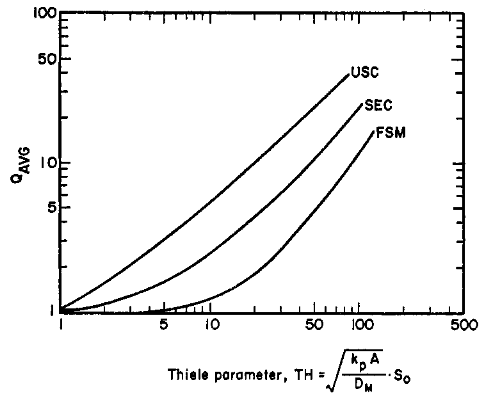

Figure 3. Q factors for three models as a function of the Theile parameter (Q at $S^* = 1.00625$ for SEC, USC; $Q_{\min}$ for FSM).

Heterogeneity of catalytic sites also has quite often been offered as an explanation for the broad molecular weight distributions of heterogeneously catalyzed polymerizations.[8] It is assumed that catalyst sites of varying activity are present, resulting in a broader distribution. The distribution so obtainable would certainly depend on the assumed distribution of catalytic site activity.

In the absence of any direct data, it appears reasonable to use a distribution function based on a Freundlich-type adsorption isotherm, such as the one derived by Sips.[18] Calculations made by using this distribution function give Q values not very far from 2. It should indeed be possible to derive alternate distribution functions for site activities which could lead to Q values of desired magnitude. Such distribution functions, however, will be much broader than the one suggested by Sips[18] and broader than those normally found for heterogeneous catalytic surfaces. Therefore, even though heterogeneity does cause broadness of molecular weight distributions, it seems that heterogeneity alone cannot account for the extremely broad distributions found in polymers produced by Ziegler–Natta catalysts.

Correlation of Kinetic Data

In Figure 4 are depicted the dimensionless rates of reaction (as effectiveness factor, ϵ) for FSM and USC models. The rates for the SEC model could lie anywhere in between, depending on the nature of the catalytic site movement, which probably is affected by the initial concentration of catalyst in the liquid phase, the degree of grinding of the catalyst and its time of aging, the amount of stirring, agglomeration of growing particles, etc. (Plans for a microscopic study of site movement are in progress.) The rate has been calculated by assuming rate of diffusion of monomer equal to the rate of reaction, *i.e.*

$$R_p' = D_M \left.\frac{\partial C_M}{\partial r}\right|_{r=S} 4\pi S^2 \text{ mol/sec} \qquad (30)$$

This rate can conveniently be rendered dimensionless by dividing by $(k_P C_S A_0)[(^4/_3)\pi S_0^3]$. In dimensionless form, the rate depends upon the Thiele parameter, the dimensionless particle diameter S^* (which is also an indication of the extent of reaction), and the dimensionless concentration gradient at the surface $\partial C_M^*/\partial r^*$. However, most of the rates re-

---

[17] L. Collatz, "The Numerical Treatment of Differential Equations," Springer-Verlag, New York, N. Y., 1966.

[18] R. Sips, *J. Chem. Phys.*, **16**, 490 (1948).

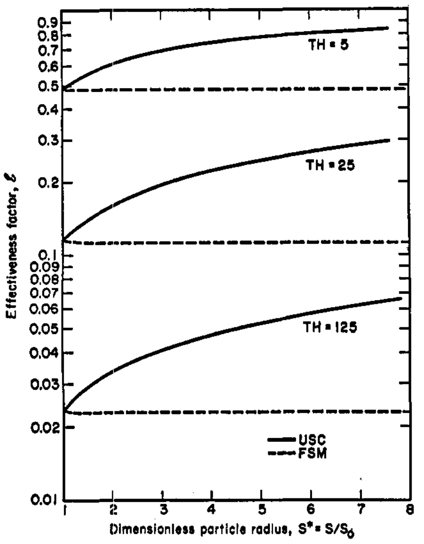

Figure 4. Effectiveness factors for two limiting cases as a function of particle growth and the Thiele parameter.

ported in the literature are per gram of catalyst. Converting R_p' to similar units

$$R_p'' = \frac{D_M \dfrac{\partial C_M}{\partial r}\Big|_{r=S} 4\pi S^2}{[(4/3)\pi S_0^3]\rho_{cst}} = 3\frac{D_M}{\rho_{cst}S_0^2} C_S \frac{\partial C_M^*}{\partial r^*}\Big|_{r^*=S^*} \tag{31}$$

where ρ_{cst} is an effective density of the polymeric core at $S = S_0$ in grams of catalyst per unit volume. Equation 31 is multiplied and divided by $(k_P A_0)$ to give a dimensionless effectiveness factor as the parameter of the equation.

$$R_p = \frac{(k_P A_0 C_S)}{\rho_{cst}} \frac{3S^{*2}}{(Th)^2} \frac{\partial C_M^*}{\partial r^*}\Big|_{r^*=S^*} = \frac{(k_P A_0 C_S)}{\rho_{cst}} \epsilon \tag{32}$$

where ϵ is an effectiveness factor and is given by

$$\epsilon = \frac{3S^{*2}}{(Th)^2} \frac{\partial C_M}{\partial r^*}\Big|_{r^*=S^*} \tag{33}$$

This effectiveness factor, ϵ, is plotted *vs.* S^* for both FSM and USC for various values of Thiele parameter in Figure 4. Almost all reported data on rates of reaction are likely to fall within these two limits; so would the rates for SEC, the exact shape and location of curve depending upon experimental conditions. A slight decline in rate may also be caused by a slight deactivation of sites or a change in diffusivity of monomer with molecular weight of polymer, both of which have been ignored in this analysis.

Figure 5 shows the particle growth rates computed from the USC model. Unfortunately, no literature data exist on these growth rates and hence a comparison with experimental results is not possible. These curves, however, are very useful in explaining the apparent anomaly in the order of reaction.

The theoretical order of reaction with respect to monomer can easily be computed by plotting the rate of reaction *vs.* monomer concentration and taking the slope of the curve. However, in order to be able to compare this order of reaction with those reported in Table I, it is more meaningful to make

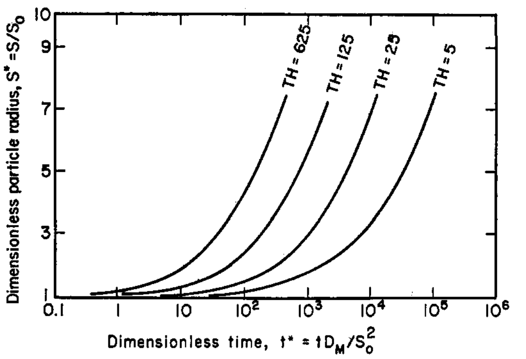

Figure 5. Particle growth curves (USC) for various values of the Thiele parameter.

plots of rate of reaction *vs.* particle diameter for various values of C_S^*, where C_S^* is C_S normalized by dividing it by an arbitrary value. This rate, in arbitrary units, is plotted in Figure 6 for the USC model (for *Th* = 25). Superimposed upon this are the particle growth curves for the same value of the Thiele parameter, so as to give lines of constant time (dimensionless), or isochrones.

The apparent order of reaction can be computed from these curves by taking the rates of reaction at two values of C_S^* and comparing the ratio of rates with the ratio of the two values of C_S^*. This may be done for various values of C_S^* to check for consistency. It can be seen from these curves that the apparent order of reaction would have a significant dependence upon where and how these rates are measured. If the rates are measured along the intersection of a vertical line with the rate curves, the ratio of rates is proportional to the first power of the ratio of concentrations, thereby giving an apparent order of reaction of unity. The vertical lines represent lines of constant S^*, and, therefore, lines of constant extent of reaction. Such data were taken by Fielchenfeld and Jeselson[19] and, as reported in Table I, the order of the reaction is unity. If instead the rates are measured at constant time, *i.e.*, along the isochrones in Figure 6, the ratio of rates is proportional to a power greater than unity of the ratio of the various values of C_S^*. This is reflected in the data of Schindler,[20,21] Natta,[22] and Vesely,[23] as shown in Table I.

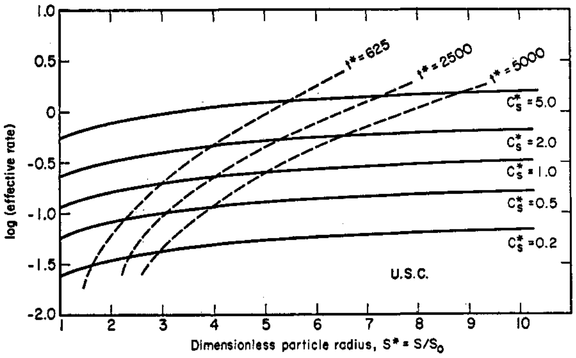

Figure 6. Rate of reaction and isochronous curves for USC model, Thiele parameter = 25.

---

(19) H. Fielchenfeld and M. Jeselson, *J. Phys. Chem.*, **63**, 720 (1959).

(20) A. Schindler, *J. Polym. Sci., Part C*, No. **4**, 81 (1964).

(21) A. Schindler, *Makromol. Chem.*, 70, 94 (1963).

(22) G. Natta, I. Pasquon, J. Swab, and A. Zambelli, *Chim. Ind. (Milan)*, **44**, 621 (1962).

(23) K. Vesely, J. Ambroz, and O. Hamrik, *J. Polym. Sci., Part C*, No. **4**, 11 (1963).

Table II
Additives Used to Narrow the MWD of Polyethylene Produced by the Ziegler–Natta Catalyst, $TiCl_4 + Al(i\text{-}C_4H_9)_3$

Patent	Additive	Patent	Additive
U. S. 3,150,122 (1964)	Phenol	U. S. 3,163,611 (1964)	Alcohol
U. S. 3,163,611 (1964)	Aldehyde	British 841,718 (1960)	Thiophenol

If the rates are measured very far to the right, *i.e.*, at steady state, the rate curves become horizontal and it becomes immaterial whether one measures the rates along a vertical or slanting line. The order of reaction at steady state, therefore, will be unity, as reported by Natta and Pasquon.[12] Ludlom and coworkers[24] did not specifically strive for a steady state nor do they make any mention of a steady state in their paper, but a close examination of their rate of ethylene consumption curves indicates that they were operating almost under steady-state conditions; hence a unity order of reaction. From the above discussion it is also obvious that a worker measuring orders of reaction over long periods of time is bound to observe a transition from second to first as he approaches the steady-state region. Such a transition was reported by Schindler,[21] though the importance of steady state was not clearly realized. The kinetic data thus appear to be in conformity with the diffusion-controlled mechanism proposed.

Design for Narrow Molecular Weight Distributions

On the basis of the above analysis, it appears that the width of the molecular weight distributions can be decreased if the monomer can be made to bypass a site near the surface and instead go to an inner site. The easiest way to achieve this is by ''killing'' the site near the surface once it has acquired a sufficient degree of polymerization. It is known that compounds like water, alcohol, etc., containing an active hydrogen are capable of terminating a Ziegler–Natta polymerization reaction. If used in limited quantities, therefore, these could be used to deactivate the sites near the surface, thereby allowing the monomer to penetrate further inside. This should result in a narrower molecular weight distribution. At least three patents claim the use of such a technique, as shown in Table II.

As the polymer particle grows, more and more sites in the central core get starved of monomer. More monomer could be made to reach some of these sites by steadily increasing the monomer pressure, thereby effecting a slight improvement in the molecular weight distribution.

An apparently promising technique is the use of a better solvent so as to increase the diffusion rate within the polymer bead. An increase in temperature may also enhance the solubility, but is likely to increase the value of the Thiele parameter simultaneously. Besides, from the work of Olivé and Olivé,[25] it appears that solubility affects stereoregularity and may cause branching of the polymer. Furthermore, there is one conjecture that the mechanism in the case of soluble polymers may not be the same[26] as for an insoluble product. Further investigations on the effects of solvents such as CCl_4, decalin, xylenes, etc., on the stereoregularity (or linearity in case of polyethylene) and the molecular weight and its distribution are necessary before anything conclusive can be said about the usefulness of this technique.

In summary, diffusion is one possible explanation for the spread in molecular weight distributions observed in Ziegler–Natta polymerizations, and the observed anomalies in the apparent order of reaction. It can lead to a molecular weight distribution at least as wide as those reported. A better understanding of this mechanism could lead to newer ways for production of narrowly dispersed polymers.

Nomenclature

a	empirical constant in eq 1
A	concentration of catalytic sites at any instant, sites/cm^3
A_0	initial concentration of catalytic sites, sites/cm^3
b	empirical constant in eq 1
C_M	concentration of monomer in the growing particle, mol/cm^3
C_M^*	$= C_M/C_S$, dimensionless monomer concentration
C_S	bulk concentration of monomer, mol/cm^3
C_S^*	$= C_S/C_S^0$, normalized bulk concentration of monomer
C_S^0	arbitrary value of monomer concentration, mol/cm^3
D_M	diffusivity of monomer
ϵ	effectiveness factor
$I(M)$	weight fraction of polymer with molecular weight less than M
k_P	rate constant for propagation reaction, cm^3/(sites sec)
k_T	rate constant for transfer reaction, cm^3/(sites sec)
M	molecular weight
M_0	parameter in eq 2
$\bar{M}_n$	number-average molecular weight
$\bar{M}_w$	weight-average molecular weight
P_i	concentration of dead i-mer, mol/cm^3
QX_{av}	as defined in eq 10
QY_{av}	as defined in eq 11
Q_{av}	as defined in eq 12
r	radius
r^*	r/S_0, dimensionless radius
R_i	concentration of living i-mers, mol/cm^3
R_p	rate of reaction, dimensionless
R_p'	rate of diffusion of monomer into particle, mol/sec
R_p''	rate of reaction, mol/(sec g of catalyst)
S	radius of particle at any instant, cm
S^*	$= S/S_0$, dimensionless particle radius
S_0	initial radius of particle, cm
Th	Thiele parameter
t	time, sec
t^*	$= tD_M/S_0^2$, dimensionless time
V_R	velocity of sites, cm/sec
X_n	local nth moment of living polymer
$X_{n,av}$	as defined in eq 8
Y_n	local nth moment of dead polymer
$Y_{n,av}$	as defined in eq 9
β	empirical constant in eq 2
ρ_{cst}	density of particles at $S = S_0$, g of catalyst/cm^3
$\Sigma_{n,av}$	total concentration of polymer, mol/cm^3

Acknowledgment. This work was supported by National Science Foundation Grant No. NSF GK 4577. Thanks are due Professor M. C. Williams for his comments on the manuscript.

---

(24) D. B. Ludlom, A. W. Anderson, and C. E. Ashby, *J. Amer. Chem. Soc.*, **80**, 1380 (1958).

(25) G. H. Olivé and S. Olivé, *J. Polym. Sci., Part B*, **8**, 205 (1970).

(26) N. M. Chitkov, *Kinet. Katal.*, **11**, 321 (1970).